

Non-Homophilic Graph Pre-Training and Prompt Learning

Xingtong Yu*

Singapore Management University
Singapore
starlien0905@gmail.com

Yuan Fang†

Singapore Management University
Singapore
yfang@smu.edu.sg

Jie Zhang*

National University of Singapore
Singapore
jiezhang_jz@u.nus.edu

Renhe Jiang†

The University of Tokyo
Japan
jiangrh@csis.u-tokyo.ac.jp

Abstract

Graphs are ubiquitous for modeling complex relationships between objects across various fields. Graph neural networks (GNNs) have become a mainstream technique for graph-based applications, but their performance heavily relies on abundant labeled data. To reduce labeling requirement, pre-training and prompt learning has become a popular alternative. However, most existing prompt methods do not differentiate homophilic and heterophilic characteristics of real-world graphs. In particular, many real-world graphs are *non-homophilic*, not strictly or uniformly homophilic with mixing homophilic and heterophilic patterns, exhibiting varying non-homophilic characteristics across graphs and nodes. In this paper, we propose PRONoG, a novel pre-training and prompt learning framework for such non-homophilic graphs. First, we analyze existing graph pre-training methods, providing theoretical insights into the choice of pre-training tasks. Second, recognizing that each node exhibits unique non-homophilic characteristics, we propose a conditional network to characterize the node-specific patterns in downstream tasks. Finally, we thoroughly evaluate and analyze PRONoG through extensive experiments on ten public datasets.

CCS Concepts

• Information systems → Web mining; Data mining; • Computing methodologies → Learning latent representations.

Keywords

Graph mining, non-homophilic graph, prompt learning, pre-training, few-shot learning.

ACM Reference Format:

Xingtong Yu*, Jie Zhang*, Yuan Fang†, and Renhe Jiang†. 2018. Non-Homophilic Graph Pre-Training and Prompt Learning. In *Proceedings of Make sure to*

*Co-first authors. Work was done while at the University of Tokyo.

†Corresponding authors.

Permission to make digital or hard copies of all or part of this work for personal or classroom use is granted without fee provided that copies are not made or distributed for profit or commercial advantage and that copies bear this notice and the full citation on the first page. Copyrights for components of this work owned by others than the author(s) must be honored. Abstracting with credit is permitted. To copy otherwise, or republish, to post on servers or to redistribute to lists, requires prior specific permission and/or a fee. Request permissions from permissions@acm.org.

Conference acronym 'XX, June 03–05, 2018, Woodstock, NY

© 2018 Copyright held by the owner/author(s). Publication rights licensed to ACM.

ACM ISBN 978-1-4503-XXXX-X/18/06
https://doi.org/XXXXXXX.XXXXXXX

enter the correct conference title from your rights confirmation email (Conference acronym 'XX). ACM, New York, NY, USA, 15 pages. <https://doi.org/XXXXXXX.XXXXXXX>

1 Introduction

Graph data are pervasive in real-world applications, such as citation networks [18, 56], social networks [16, 68], and molecular graphs [21, 51]. Traditional methods typically train graph neural networks (GNNs) [20, 47] or graph transformers [59, 66] in a supervised manner. However, they require re-training and substantial labeled data for each specific task.

To mitigate the limitations of supervised methods, pre-training methods have gained significant traction [15, 36, 48, 60]. They first learn universal, task-independent properties from unlabeled graphs, and then fine-tune the pre-trained models to various downstream tasks using task-specific labels [48, 60]. However, a significant gap occurs between the pre-training objectives and downstream tasks, resulting in suboptimal performance [44, 61]. Moreover, fine-tuning large pre-trained models is costly and still requires sufficient task-specific labels to prevent overfitting. As an alternative to fine-tuning, prompt learning has emerged as a popular parameter-efficient technique for adaptation to downstream tasks [7, 26, 42, 43, 46, 62]. They first utilize a universal template to unify pre-training and downstream tasks. Then, a learnable prompt is employed to modify the input features or hidden embeddings of the pre-trained model to align with the downstream task without updating the pre-trained weights. Since a prompt has far fewer parameters than the pre-trained model, prompt learning can be especially effective in low-resource settings [61].

However, current graph “pre-train, prompt” approaches rely on the homophily assumption or overlook the presence of heterophilic edges. Specifically, the homophily assumption [29, 75] states that neighboring nodes should share the same labels, whereas heterophily refers to the opposite scenario where two neighboring nodes have different labels. We observe that real-world graphs are typically *non-homophilic*, meaning they are *neither strictly or uniformly homophilic* and mix *both homophilic and heterophilic patterns* [54, 55]. In this work, we investigate the pre-training and prompt learning methodology for non-homophilic graphs. We first revisit existing graph pre-training methods for such graphs, followed by proposing a **Prompt** learning framework for Non-homophilic Graphs (or PRONoG in short). The solution is non-trivial, as the notion of homophily encompasses two key aspects, each with its own unique challenge.

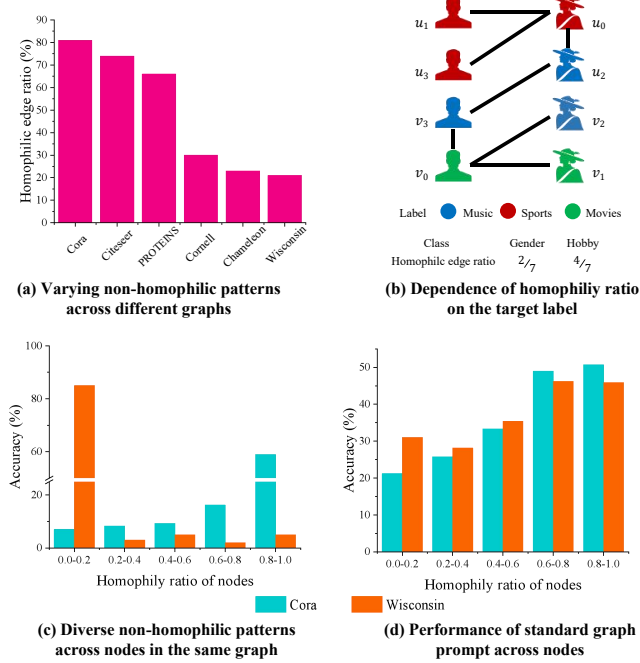


Figure 1: Non-homophilic characteristics of graphs.

First, different graphs exhibit varying degrees of non-homophily. As shown in Fig. 1(a), the *Cora* citation network that is generally considered largely homophilic with 81% homophilic edges¹, whereas the *Wisconsin* webpage graph links different kinds of webpages, which is highly heterophilic with only 21% homophilic edges. Moreover, the non-homophilic characteristics of a graph also depends on the target label. For example, in a dating network shown in Fig. 1(a), taking gender as the node label, the graph is more heterophilic with 2/7 homophilic edges. However, taking hobbies as the node label, the graph becomes more homophilic with 4/7 homophilic edges. Hence, *how do we pre-train a graph model irrespective of the graph's homophily characteristics?* In this work, we propose definitions for *homophily tasks* and *homophily samples*. We show that pre-training with non-homophily samples increases the loss of any homophily task. Meanwhile, a less homophilic graph results in a higher number of non-homophily samples, subsequently increasing the pre-training loss for homophily tasks. This motivates us to move away from homophily tasks for graph pre-training [26, 42] and instead choose a non-homophily task [54, 60].

Second, different nodes within the same graph are distributed differently in terms of their non-homophilic characteristics. As shown in Fig. 1(c), on both *Cora* and *Cornell*, their nodes have a diverse homophily ratios². Hence, *how do we capture the fine-grained, node-specific non-homophilic characteristics?* Due to the diverse characteristics across nodes, a one-size-fits-all solution for all nodes would be inadequate. However, existing approaches generally apply a single prompt to all nodes [7, 26, 42, 43], treating all nodes uniformly. Thus, these methods overlook the fine-grained node-wise non-homophilic characteristics, leading to suboptimal

¹Defined as edges connecting two nodes of the same label; see Eq. (1) in Sect. 3.

²Defined as the fraction of a node's neighbors with the same label; see Eq. (2) in Sect. 3.

performance. For example, a standard graph prompt learning approach [26] generally performs worse when the homophily ratios of nodes decrease, as shown in Fig. 1(d), even with a non-homophily pretext task [60]. Though some recent works [5, 46] have proposed node-specific prompts, they are not designed to account for the variation in nodes' non-homophilic characteristics. Inspired by conditional prompt learning [71], we propose generating a unique prompt from each node with a conditional network (condition-net) to capture the fine-grained, distinct characteristics of each node. We first capture the non-homophilic patterns of each node by reading out its multi-hop neighborhood. Then, conditioned on these non-homophilic patterns, the condition-net produces a series of prompts, one for each node that reflects its varying non-homophilic characteristics. These prompts can adjust the node embeddings to better align them with the downstream task.

In summary, the contributions of this work are threefold: (1) We observe varying degrees of homophily across graphs, which motivates us to revisit graph pre-training tasks. We provided theoretical insights which guide us to choose non-homophily tasks for graph pre-training. (2) We further observe that, within the same graph, different nodes have diverse distributions of non-homophilic characteristics. To adapt to the unique non-homophilic patterns of each node, we propose the ProNoG framework for non-homophilic prompt learning, which is equipped with a condition-net to generate a series of prompts conditioned on each node. The node-specific prompts enables fine-grained, node-wise adaptation for the downstream tasks. (3) We perform extensive experiments on ten benchmark datasets, demonstrating the superior performance of ProNoG compared to a suite of state-of-the-art methods.

2 Related Work

Graph representation learning. GNNs [11, 20, 47, 57, 63] are mainstream technique for graph representation learning. They typically operate on a message-passing framework, where nodes iteratively update their representations by aggregating messages received from their neighboring nodes. However, the effectiveness of GNNs heavily relies on abundant task-specific labeled data and requires re-training for various tasks. Inspired by the success of pre-training methods in the language [4, 6, 9, 40] and vision [1, 67, 71, 72] domains, pre-training methods [14, 15, 19, 27, 36, 45, 48, 60] have been widely explored for graphs. These methods first pre-train a graph encoder based on self-supervised tasks, then transfer prior knowledge to downstream tasks. However, all these GNNs and pre-training methods are based on the homophilic assumption, overlooking that real-world graphs are generally non-homophilic.

Non-homophilic graph learning. Many GNNs [2, 28, 29, 35, 73–75] have been proposed for non-homophilic graphs, employing methods such as capturing high-frequency signals [2], discovering potential neighbors [17, 33], and high-order message passing [75]. Moreover, recent works have explored pre-training on non-homophilic graphs [13, 54, 55] by capturing neighborhood information to construct unsupervised tasks for pre-training the graph encoder and then transferring prior non-homophilic knowledge to downstream tasks through fine-tuning with task-specific supervision. However, a significant gap exists between the objectives

of pre-training and fine-tuning [23, 44, 61]. While pre-training focuses on learning inherent graph attributes without supervision, fine-tuning adapts these insights to downstream tasks based on task-specific supervision. This discrepancy hinders effective knowledge transfer and negatively impacts downstream performance.

Graph prompt learning. Originally developed for the language domain, prompt learning effectively unifies pre-training and downstream objectives [4, 22, 24]. Recently, graph prompt learning has emerged as a popular alternation to fine-tuning methods [7, 26, 42, 43, 46, 62, 64]. These methods first propose a unified template, then design prompts specifically tailored to each downstream task, allowing them to better align with the pre-trained model while keeping the pre-trained parameters frozen. However, current graph prompt learning methods typically assume graphs are homophilic [43, 61], neglecting the fact that real-world graphs are generally non-homophilic, exhibiting a mixture of homophilic and heterophilic patterns. Furthermore, these methods usually apply a single prompt for all nodes, overlooking the unique characteristics of each node's non-homophilic pattern.

3 Preliminaries

Graph. A graph is defined as $G = (V, E)$, where V represents the set of nodes and E represents the set of edges. The nodes are also associated with a feature matrix $\mathbf{X} \in \mathbb{R}^{|V| \times d}$, such that $\mathbf{x}_v \in \mathbb{R}^d$ is a row of \mathbf{X} representing the feature vector for node $v \in V$. For a collection of multiple graphs, we use the notation $\mathcal{G} = \{G_1, G_2, \dots, G_N\}$.

Homophily ratio. Given a mapping between the nodes of a graph and a predefined set of labels, let y_v denote the label mapped to node v . The homophily ratio $\mathcal{H}(G)$ evaluates the relationships between the labels and the graph structure [29, 75], measuring the fraction of homophilic edges whose two end nodes share the same label. More concretely,

$$\mathcal{H}(G) = \frac{|\{(u, v) \in E : y_u = y_v\}|}{|E|}. \quad (1)$$

Additionally, the homophily ratio can be defined for each node based on its local structure [30, 55], measuring the fraction of a node's neighbors that share the same label. This node-specific ratio can be defined as

$$\mathcal{H}(v) = \frac{|\{u \in \mathcal{N}(v) : y_u = y_v\}|}{|\mathcal{N}(v)|}, \quad (2)$$

where $|\mathcal{N}(v)|$ is the set of neighboring nodes of v . Note that both $\mathcal{H}(G)$ and $\mathcal{H}(v)$ are in $[0, 1]$. Graphs or nodes with a larger proportion of homophilic edges have a higher homophily ratio.

Graph encoder. Graph encoders learn latent representations of graphs, embedding their nodes into some feature space. A widely used family of graph encoders is GNNs, which typically utilize a message-passing mechanism [53, 70]. Specifically, each node aggregates messages from its neighbors to generate its own representation. By stacking multiple layers, GNNs enables recursive message passing throughout the graph. Formally, the embedding of a node v in the l -th GNN layer, denoted as \mathbf{h}_v^l , is computed as follows.

$$\mathbf{h}_v^l = \text{Aggr}(\mathbf{h}_v^{l-1}, \{\mathbf{h}_u^{l-1} : u \in \mathcal{N}(v)\}; \theta^l), \quad (3)$$

where θ^l are the learnable parameters in the l -th layer, and $\text{Aggr}(\cdot)$ is the aggregation function, which can take various forms [11, 20, 47, 57, 63]. In the first layer, the input node embedding \mathbf{h}_v^0 is typically initialized from the node feature vector \mathbf{x}_v . The full set of learnable parameters is denoted as $\Theta = \{\theta^1, \theta^2, \dots\}$. For simplicity, we define the output node representations of the final layer as \mathbf{h}_v , which can then be fed into the loss function for a specific task.

Problem statement. In this work, we aim to pre-train a graph encoder and develop a prompt learning framework for non-homophilic graphs. More specifically, both the pre-training and prompt learning are not sensitive to the homophilic characteristics of the graph and its nodes.

To evaluate our non-homophilic pre-training and prompt learning, we focus on two common tasks on graph data: node classification and graph classification, in few-shot settings. For node classification within a graph $G = (V, E)$, let Y be the set of node classes. Each node $v_i \in V$ has a class label $y_i \in Y$. Similarly, for graph classification across a set of graphs \mathcal{G} , let \mathcal{Y} be the set of possible graph labels. Each graph $G_i \in \mathcal{G}$ has a class label $Y_i \in \mathcal{Y}$. In the few-shot setting, there are only k labeled samples per class, where k is a small number (e.g., $k \leq 10$). This scenario is known as k -shot classification [26, 62, 65]. Note that the homophily ratio is defined with respect to some predefined set of labels, which may not be related to the class labels in downstream tasks.

4 Revisiting Graph Pre-training

In this section, we revisit graph pre-training tasks to cope with non-homophilic graphs. We first propose the definition of *homophily tasks* and reveal its connection to the training loss. The theoretical insights further guide us in choosing graph pre-training tasks.

4.1 Theoretical Insights

We focus on contrastive graph pre-training tasks. Given a mainstream contrastive task [12, 26, 36, 60, 62, 76], $T = (\{\mathcal{A}_u : u \in V\}, \{\mathcal{B}_u : u \in V\})$, its loss function \mathcal{L}_T can be generalized to a standard form below.

$$\mathcal{L}_T = - \sum_{u \in V} \ln P(u, \mathcal{A}_u, \mathcal{B}_u), \quad (4)$$

$$P(u, \mathcal{A}_u, \mathcal{B}_u) \triangleq \frac{\sum_{a \in \mathcal{A}_u} \text{sim}(\mathbf{h}_u, \mathbf{h}_a)}{\sum_{a \in \mathcal{A}_u} \text{sim}(\mathbf{h}_u, \mathbf{h}_a) + \sum_{b \in \mathcal{B}_u} \text{sim}(\mathbf{h}_u, \mathbf{h}_b)}, \quad (5)$$

where $\text{sim}(\cdot, \cdot)$ represents a similarity function such as cosine similarity [37] in our experiment, \mathcal{A}_u is the set of positive instances for node u , and \mathcal{B}_u is the set of negative instances for u . The optimization objective of task T in Eq. (4) is to maximize the similarity between u and its positive instances while minimizing the similarity between u and its negative instances. Based on this loss, we further propose the definitions of *homophily tasks* and *homophily samples*.

DEFINITION 1 (HOMOPHILY TASK). *On a graph $G = (V, E)$, a pre-training task $T = (\{\mathcal{A}_u : u \in V\}, \{\mathcal{B}_u : u \in V\})$ is a homophily task if and only if, $\forall u \in V, \forall a \in \mathcal{A}_u, \forall b \in \mathcal{B}_u, (u, a) \in E \wedge (u, b) \notin E$. A task that is not a homophily task is called a non-homophily task.* \square

In particular, the widely used link prediction task [26, 32, 34, 62, 64, 65] is a homophily task, where \mathcal{A}_u is a subset of nodes linked to u and \mathcal{B}_u is a subset of nodes not linked to u .

DEFINITION 2 (HOMOPHILY SAMPLE). On a graph $G = (V, E)$, consider a triplet (u, a, b) where $u \in V$, $(u, a) \in E$ and $(u, b) \notin E$. The triplet (u, a, b) is a homophily sample if and only $\text{sim}(u, a) > \text{sim}(u, b)$, and it is a non-homophily sample otherwise. \square

Subsequently, we can establish the following theorems.

THEOREM 1. For a homophily task T , adding a homophily sample always results in a smaller loss than adding a non-homophily sample.

PROOF. Consider a homophily sample (u, a, b) for some $(u, a) \in E$ and $(u, b) \notin E$, as well as a non-homophily sample (u, a', b') for some $(u, a') \in E$ and $(u, b') \notin E$. Let the overall loss with (u, a, b) be L_T , and that with (u, a', b') be L'_T . Since (u, a, b) is homophily, we have $\text{sim}(u, a) > \text{sim}(u, b)$, and thus $p(u, a, b) > 0.5$. Moreover, since (u, a', b') is non-homophily, we have $\text{sim}(u, a') \leq \text{sim}(u, b')$, and thus $p(u, a', b') \leq 0.5$. Hence, $p(u, a, b) > p(u, a', b')$, implying that $L_T < L'_T$. \square

THEOREM 2. Consider a graph $G = (V, E)$ with a label mapping function $V \rightarrow Y$, and let $y_v \in Y$ denote the label mapped to $v \in V$. Suppose the label mapping satisfies that

$$\forall u, a, b \in V, y_u = y_a \wedge y_u \neq y_b \Rightarrow \text{sim}(u, a) > \text{sim}(u, b).$$

Let \mathbb{E}_T denote the expected number of homophily samples for a homophily task T on the graph G . Then, \mathbb{E}_T increases monotonically as the homophily ratio $\mathcal{H}(G)$ defined w.r.t. Y increases.

PROOF. For a homophily task $T = (\{\mathcal{A}_u : u \in V\}, \{\mathcal{B}_u : u \in V\})$, a triplet (u, a, b) for some $u \in V$, $a \in \mathcal{A}_u$ and $b \in \mathcal{B}_u$ is a homophily sample with a probability of $P(y_u = y_a)(1 - P(y_u = y_b))$, since $y_u = y_a \wedge y_u \neq y_b$ implies $\text{sim}(u, a) > \text{sim}(u, b)$. Hence, the expected number of homophily samples for T is

$$\mathbb{E}_T = \sum_{u \in V} |\mathcal{A}_u| |\mathcal{B}_u| P(y_u = y_a)(1 - P(y_u = y_b)). \quad (6)$$

For a constant number of nodes with label y_u , as $\mathcal{H}(G)$ increases, $P(y_u = y_a)$ always increases while $P(y_u = y_b)$ always decreases, leading to a larger \mathbb{E}_T . \square

In the next part, the theorems will guide us in choosing the appropriate pre-training tasks for non-homophilic graphs.

4.2 Non-homophilic Graph Pre-training

Consider a homophily task T . According to Theorem 2, for non-homophilic graphs with lower homophily ratios, on average there are fewer homophily samples and more non-homophily samples for T . Consequently, based on Theorem 1, adding a non-homophily sample always results in a larger loss than adding a homophily sample. Therefore, for non-homophilic graphs, especially those with low homophily ratio, non-homophily tasks are a better choice compared to homophily tasks when optimizing the training loss.

We revisit mainstream graph pre-training methods and categorize them into two categories: homophily methods that employ homophily tasks, and non-homophily methods that do not. Specifically, GMI [34], GraphPrompt [26], MultiGPrompt [65], HGPrompt [64] and GraphPrompt+ [62] are all homophily methods, since their pre-training tasks utilizes a form of link prediction, where \mathcal{A}_u is a set of nodes linked to u , and \mathcal{B}_u is a set of nodes not linked from u . In contrast, DGI [48], GraphCL [60], and GraphACL [55] are

non-homophily methods, since \mathcal{A}_u and \mathcal{B}_u in their pre-training tasks are not related to the connectivity with u . Further details of these methods are shown in Appendix B. In our experiment, we use the non-homophily method GraphCL as the pretext task to obtain our main results for non-homophily graphs, as it is a classic pre-training method with competitive performance. We also experiment with link prediction [26] and GraphACL for further evaluation, as shown in Table 5.

5 Non-homophilic Prompt Learning

In this section, we propose ProNoG, our prompt learning framework for non-homophilic graphs. We first introduce the overall framework, and then develop the prompt generation and tuning process. Finally, we present the overall algorithm and analyze its complexity.

5.1 Overall framework

We illustrate the overall framework of ProNoG in Fig. 2. It involves two stages: (a) graph pre-training and (b) downstream adaptation. In graph pre-training, we pre-train a graph encoder using a non-homophilic pre-training task, as shown in Fig. 2(a). Subsequently, to adapt the pre-trained model to downstream tasks, we propose a conditional network (condition-net) that generates a series of prompts, as depicted in Fig. 2(b). As a result, each node is equipped with its own prompt, which can be used to modify its features to align with the downstream task. More specifically, the prompt generation is conditioned on the unique patterns of each node, in order to achieve fine-grained adaptation catering to the diverse non-homophilic characteristics of each node, as detailed in Fig. 2(c).

5.2 Prompt Generation and Tuning

Prompt generation. In non-homophilic graphs, different nodes are characterized by unique non-homophilic patterns. Specifically, different nodes typically have diverse homophily ratios $\mathcal{H}(v)$, indicating distinct topological structures linking to their neighboring node. Moreover, even nodes with similar homophily ratios may have different neighborhood distributions in terms of the varying homophily ratios of the neighboring nodes. Therefore, instead of learning a single prompt for all nodes as in standard graph prompt learning [26, 42, 43, 62], we design a condition-net [71] to generate a series of non-homophilic pattern-conditioned prompts. Consequently, each node is equipped with its own unique prompt, aiming to adapt to its distinct non-homophilic characteristics.

First, the non-homophilic patterns of a node can be characterized by considering a multi-hop neighborhood around the node. Specifically, given a node v , we readout their δ -hop ego-network S_v , which is an induced subgraph containing the node v and nodes reachable from v in at most δ steps. Inspired by GGCN [58], the readout is weighted by the similarity between v and their neighbors, as shown in Fig. 2(c), obtaining a representation of the subgraph S_v given by

$$\mathbf{s}_v = \frac{1}{|S_v|} \sum_{u \in S_v} \mathbf{h}_u \cdot \text{sim}(\mathbf{h}_u, \mathbf{h}_v), \quad (7)$$

where $|S_v|$ denotes the number of nodes in S_v . In our experiment, we set $\delta = 2$ to balance between efficiency and capturing more unique non-homophilic patterns in the neighborhood of v .

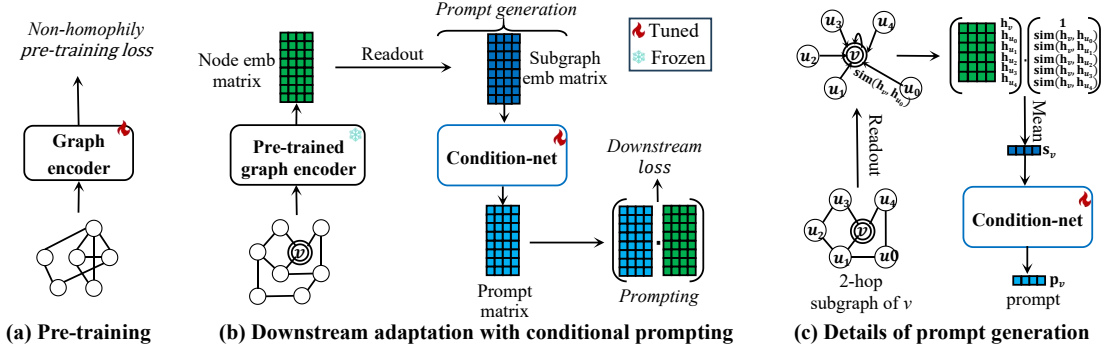


Figure 2: Overall framework of PRONoG.

Next, for each downstream task, our goal is to assign a unique prompt vector to each node. However, directly parameterizing these prompt vectors would significantly increase the number of learnable parameters, which may overfit to the lightweight supervision in few-shot settings. To cater to the unique non-homophilic characteristics of each node with minimal parameters, we propose to employ a condition-net [71] to generate node-specific prompt vectors. Specifically, conditioned on the subgraph readout s_v of a node v , the condition-net generates a unique prompt vector for v w.r.t. a task t , denoted by $p_{t,v}$, as follows.

$$p_{t,v} = \text{CondNet}(s_v; \phi_t), \quad (8)$$

where CondNet is the condition-net parameterized by ϕ_t . It outputs a unique prompt vector $p_{t,v}$, which varies based on the input s_v that characterizes the non-homophily patterns of node v . Note that this is a form of hypernetworks [10], which employs a secondary network to generate the parameters for the main network conditioned on the input feature. In our context, the condition-net is the secondary network, generating prompt parameters without expanding the number of learnable parameters in the main network. The secondary network CondNet can be any learnable function, such as a fully-connected layer or a multi-layer perceptron (MLP). We employ an MLP with a compact bottleneck architecture [52].

Subsequently, we perform fine-grained, node-wise adaptation to task t . Concretely, the prompt $p_{t,v}$ for node v is employed to adjust v 's features or its embeddings in the hidden or output layers [62]. In our experiments, we choose a simple yet effective implementation that modifies the nodes' output embeddings through an element-wise product, as follows.

$$\tilde{h}_{t,v} = p_{t,v} \odot h_v, \quad (9)$$

where the prompt $p_{t,v}$ is generated with an equal dimension as h_v .

Prompt tuning. In this work, we focus on two common types of downstream task: node classification and graph classification. The prompt tuning process does not directly optimize the prompt vectors; instead it optimizes the condition-net, which subsequently generates the prompt vectors, for a given downstream task.

We utilize a loss function based on node/graph similarity following previous work [26, 62]. Formally, for a task t with a labeled training set $\mathcal{D}_t = \{(x_i, y_i), (x_2, y_2), \dots\}$, where x_i can be either a node or a graph, and $y_i \in Y$ is x_i 's class label from a set of classes

Y . The downstream loss function is

$$\mathcal{L}_{\text{down}}(\phi_t) = - \sum_{(x_i, y_i) \in \mathcal{D}_t} \ln \frac{\exp\left(\frac{1}{\tau} \text{sim}(\tilde{h}_{t,x_i}, \tilde{h}_{t,y_i})\right)}{\sum_{c \in Y} \exp\left(\frac{1}{\tau} \text{sim}(\tilde{h}_{t,x_i}, \tilde{h}_{t,c})\right)}, \quad (10)$$

where \tilde{h}_{t,x_i} denotes the output embedding of node v /graph G for task t . Specifically, for node classification $\tilde{h}_{t,v}$ is the output embedding in Eq. 9; for graph classification, $\tilde{h}_{t,G} = \sum_{u \in V} \tilde{h}_{t,u}$ involving an additional graph readout. The prototype embedding for class c , $\tilde{h}_{t,c}$, is the average of the output embedding of all nodes/graphs belonging to class c .

During prompt tuning, we update only the lightweight parameters of the condition-net (ϕ_t), while freezing the pre-trained GNN weights. Thus, our prompt tuning is parameter-efficient and amenable to few-shot settings, where \mathcal{D}_t contains only a small number of training examples for task t .

5.3 Algorithm and Complexity Analysis

Algorithm. We detail the main steps for conditional prompt generation and tuning in Algorithm 1, Appendix A.

Complexity analysis. For a downstream graph G , the computational process of PRONoG involves two main parts: encoding nodes via a pre-trained GNN, and conditional prompt learning. The first part's complexity is determined by the GNN's architecture, akin to other methods employing a pre-trained GNN. In a standard GNN, each node aggregates features from up to n neighbors per layer. Assuming the aggregation involves at most D neighbors, the complexity of calculating node embeddings over L layers is $O(D^L \cdot |V|)$, where $|V|$ denotes the number of nodes. The second part, conditional prompt learning, has two stages: prompt generation and prompt tuning. In the prompt generation stage, each subgraph embedding is fed into the condition-net. In our experiment, we use a 2 layer MLP as condition-net, resulting in a complexity of $O(2 \cdot |V|)$. During prompt tuning, each node in G is adjusted using a prompt vector, with a complexity of $O(|V|)$. Therefore, the total complexity for conditional prompt learning is $O(3 \cdot |V|)$.

In conclusion, the overall complexity of PRONoG is $O((D^L + 3) \cdot |V|)$. The first part dominates the overall complexity, as $O(n^L \cdot |V|) \gg O(3 \cdot |V|)$, where we set $L = 2$ for experiments on low-homophily graphs. Thus, the additional computational cost introduced by the conditional prompt tuning step is minimal.

Table 1: Summary of datasets.

	Graphs	Homophily ratio	Graph classes	Avg. nodes	Avg. edges	Node features	Node classes
Wisconsin	1	0.21	-	251	199	1,703	5
Squirrel	1	0.22	-	5,201	217,073	2,089	5
Chameleon	1	0.23	-	2,277	36,101	2,325	5
Cornell	1	0.30	-	183	295	1,703	5
PROTEINS	1,113	0.66	2	39.06	72.82	1	3
ENZYMES	600	0.67	6	32.63	62.14	18	3
Citeseer	1	0.74	-	3,327	4,732	3,703	6
Cora	1	0.81	-	2,708	5,429	1,433	7
BZR	405	-	2	35.75	38.36	3	-
COX2	467	-	2	41.22	43.45	3	-

Homophily ratio is calculated by Eq. 1. Note that *BZR* and *COX2* do not have any node label, and thus it is not able to calculate their homophily ratios.

6 Experiments

In this section, we conduct experiments to evaluate ProNoG, and analyze the empirical results.

6.1 Experimental Setup

Datasets. We conduct experiments on ten benchmark datasets. *Wisconsin* [33], *Cornell* [33], *Chameleon* [39], and *Squirrel* [39] are all webpage graphs. Each dataset features a single graph where nodes correspond to web pages and edges represent hyperlinks connecting these pages. *Cora* [31] and *Citeseer* [41] are citation networks. These datasets consist of a single graph each, with nodes signifying scientific papers and edges indicating citation relationships. *PROTEINS* [3] consists of a series of protein graphs. Nodes in these graphs denote secondary structures, while edges depict neighboring relationships either within the amino acid sequence or in three-dimensional space. *ENZYMES* [50], *BZR* [38], and *COX2* [38] are collections of molecular graphs. These datasets describe enzyme structures from the BRENDA enzyme database, ligands related to benzodiazepine receptors, and cyclooxygenase-2 inhibitors, respectively. We summarize these datasets in Table 1, and present further details in Appendix C.

Baselines. We evaluate ProNoG against a series of state-of-the-art methods, categorized into three primary groups:

(1) *End-to-end graph neural networks*: GCN [20], GAT [47], H2GCN [75], and FAGCN [2] are trained in a supervised manner directly using downstream labels. Specifically, GCN and GAT are originally designed for homophilic graphs, H2GCN for heterophilic graphs, and FAGCN for non-homophilic graphs.

(2) *Graph pre-training models*: DGI [48], GraphCL [60], DSSL [54], GraphACL [55] follow the “pre-train, fine-tune” paradigm.

(3) *Graph prompt learning models*: GPPT [42], GraphPrompt [26], and GraphPrompt+ [62] use self-supervised pre-training tasks with a single type of prompt for downstream adaptation. Note that GPPT is specifically designed for node classification and cannot be directly used for graph classification. Therefore, in our experiments, we use GPPT exclusively for node classification tasks.

We provide further details on these baselines in Appendix D. It’s worth noting that some graph few-shot learning methods, such as Meta-GNN [69], AMM-GNN [49], RALE [25], VNT [46], and ProG

[43], are based on the meta-learning paradigm [8], which requires an additional set of labeled base classes in addition to the few-shot classes. Consequently, these methods are not directly comparable to our framework.

Parameter settings. For all baselines, we use the original authors’ code and follow their recommended settings, while further tuning their hyperparameters to ensure optimal performance. Detailed descriptions of the implementations and settings for both the baselines and our ProNoG are provided in Appendix E.

Setup of downstream tasks. We conduct two types of downstream task: *node classification*, and *graph classification*. These tasks are set up as k -shot classification problems, meaning that for each class, k instances (nodes or graphs) are randomly selected for supervision. Given that all low-homophilic datasets, i.e., *Wisconsin*, *Squirrel*, *Chameleon* and *Cornell* only comprise a single graph and cannot be directly used for graph classification. Thus, following previous research [27, 64], we generate multiple graphs by constructing ego-networks centered on the labeled nodes in each dataset. We then perform graph classification on these ego-networks, each labeled according to its central node. For datasets with high homophily ratios, *PROTEINS*, *ENZYMES*, *BZR* and *COX2* have original graph labels, so we directly conduct graph classification on these graphs. Since the k -shot tasks are balanced classification problems, we use accuracy to evaluate performance, in line with prior studies [25, 26, 49, 62]. We pre-train the graph encoder once for each dataset and then use the same pre-trained model for all downstream tasks. We generate 100 k -shot tasks for both node classification and graph classification by repeating the sampling process 100 times. Each task is executed with five different random seeds, leading to a total of 500 results per task type. We report the mean and standard deviation of these 500 outcomes.

6.2 Few-shot Performance Evaluation

We first evaluate one-shot classification tasks. Then, we vary the number of shots to investigate their impact on performance.

One-shot performance. We present the results of one-shot node and graph classification tasks on non-homophilic graphs in Tables 2 and 3, respectively. We make the following observations: (1) ProNoG surpasses all baseline methods across all settings, outperforming the best competitor by up to 21.49% on node classification and 6.50% on graph classification. These results demonstrate its effectiveness in learning prior knowledge from non-homophilic graphs and capturing nodes’ specific patterns. (2) Other graph prompt learning methods, i.e., GPPT, GraphPrompt, and GraphPrompt+, significantly lag behind ProNoG. Their suboptimal performance can be attributed to their inability to account for a variety of node-specific patterns. These results underscore the importance of our conditional prompting in characterizing node embeddings to capture nodes’ specific patterns. (3) GPPT is at best comparable to, and often performs worse than other baselines because it is not specifically designed for few-shot learning.

Few-shot performance. To assess the performance of ProNoG with different amounts of labeled data, we vary the number of shots in the downstream tasks and present the results in Fig. 3 and Appendix F. Note that given the limited number of nodes in

Table 2: Accuracy evaluation on few-shot node classification.

Methods	Wisconsin	Squirrel	Chameleon	Cornell	PROTEINS	ENZYMEs	Citeseer	Cora
GCN	21.39 \pm 6.56	20.00 \pm 0.29	25.11 \pm 4.19	21.81 \pm 4.71	43.32 \pm 9.35	48.08 \pm 4.71	31.27 \pm 4.53	28.57 \pm 5.07
GAT	28.01 \pm 5.40	21.55 \pm 2.30	24.82 \pm 4.35	23.03 \pm 13.19	31.79 \pm 20.11	35.32 \pm 18.72	30.76 \pm 5.40	28.40 \pm 6.25
H2GCN	23.60 \pm 4.64	21.90 \pm 2.15	25.89 \pm 4.96	32.77 \pm 14.88	29.60 \pm 6.99	37.27 \pm 8.73	26.98 \pm 6.25	34.58 \pm 9.43
FAGCN	35.03 \pm 17.92	20.91 \pm 1.79	22.71 \pm 3.74	28.67 \pm 17.64	32.63 \pm 9.94	35.87 \pm 13.47	26.46 \pm 6.34	28.28 \pm 9.57
DGI	28.04 \pm 6.47	20.00 \pm 1.86	19.33 \pm 4.57	32.54 \pm 15.66	45.22 \pm 11.09	48.05 \pm 14.83	45.00 \pm 9.19	54.11 \pm 9.60
GRAPHCL	29.85 \pm 8.46	21.42 \pm 2.22	27.16 \pm 4.31	24.69 \pm 14.06	46.15 \pm 10.94	48.88 \pm 15.98	43.12 \pm 9.61	51.96 \pm 9.43
DSSL	28.46 \pm 10.31	20.94 \pm 1.88	<u>27.92</u> \pm 3.93	20.36 \pm 5.38	40.42 \pm 10.08	<u>66.59</u> \pm 19.28	39.86 \pm 8.60	40.79 \pm 7.31
GRAPHACL	<u>34.57</u> \pm 10.46	<u>24.44</u> \pm 3.94	26.72 \pm 4.67	<u>33.17</u> \pm 16.06	42.16 \pm 13.50	47.57 \pm 14.36	35.91 \pm 7.87	46.65 \pm 9.54
GPPT	27.39 \pm 6.67	20.09 \pm 0.91	24.53 \pm 2.55	25.09 \pm 2.92	35.15 \pm 11.40	35.37 \pm 9.37	21.45 \pm 3.45	15.37 \pm 4.51
GRAPHPROMPT	31.48 \pm 5.18	21.22 \pm 1.80	25.36 \pm 3.99	31.00 \pm 13.88	<u>47.22</u> \pm 11.05	53.54 \pm 15.46	<u>45.34</u> \pm 10.53	<u>54.25</u> \pm 9.38
GRAPHPROMPT+	31.54 \pm 4.54	21.24 \pm 1.82	25.73 \pm 4.50	31.65 \pm 14.48	46.08 \pm 9.96	57.68 \pm 13.12	45.23 \pm 10.01	52.51 \pm 9.73
ProNoG	44.72 \pm 11.93	24.59 \pm 3.41	30.67 \pm 3.73	37.90 \pm 9.31	48.95 \pm 10.85	72.94 \pm 20.23	49.02 \pm 10.66	57.92 \pm 11.50

Results are reported in percent. The best method is bolded and the runner-up is underlined.

Table 3: Accuracy evaluation on few-shot graph classification.

Methods	Wisconsin	Squirrel	Chameleon	Cornell	PROTEINS	ENZYMEs	BZR	COX2
GCN	21.39 \pm 6.56	11.77 \pm 3.10	17.21 \pm 4.80	26.36 \pm 4.35	51.66 \pm 10.87	19.30 \pm 6.36	45.06 \pm 16.30	43.84 \pm 13.94
GAT	24.93 \pm 7.59	20.70 \pm 1.51	<u>25.71</u> \pm 3.32	22.66 \pm 12.46	51.33 \pm 11.02	20.24 \pm 6.39	46.28 \pm 15.26	51.72 \pm 13.70
H2GCN	22.23 \pm 6.38	20.69 \pm 1.42	<u>26.76</u> \pm 3.98	23.11 \pm 11.78	53.81 \pm 8.85	19.40 \pm 5.57	50.28 \pm 12.13	53.70 \pm 11.73
FAGCN	23.81 \pm 9.50	20.83 \pm 1.43	25.93 \pm 4.03	25.71 \pm 13.12	55.45 \pm 11.57	19.95 \pm 5.94	50.93 \pm 12.41	50.22 \pm 11.50
DGI	<u>29.77</u> \pm 6.22	20.50 \pm 1.52	24.29 \pm 4.33	18.60 \pm 12.79	50.32 \pm 13.47	21.57 \pm 5.37	49.97 \pm 12.63	54.84 \pm 14.76
GRAPHCL	27.93 \pm 5.27	<u>21.01</u> \pm 1.86	26.45 \pm 4.30	20.03 \pm 10.05	54.81 \pm 11.44	19.93 \pm 5.65	50.50 \pm 18.62	47.64 \pm 22.42
DSSL	22.05 \pm 3.90	20.74 \pm 1.61	26.19 \pm 3.72	18.38 \pm 10.63	52.73 \pm 10.98	<u>23.14</u> \pm 6.71	49.04 \pm 8.75	54.23 \pm 14.17
GRAPHACL	22.98 \pm 5.89	20.80 \pm 1.28	26.28 \pm 3.93	<u>26.50</u> \pm 17.18	56.11 \pm 13.95	20.28 \pm 5.60	49.24 \pm 17.87	49.59 \pm 23.93
GRAPHPROMPT	28.34 \pm 3.89	21.22 \pm 1.80	26.51 \pm 4.67	24.06 \pm 13.71	53.61 \pm 8.90	21.85 \pm 6.17	50.46 \pm 11.46	<u>55.01</u> \pm 15.23
GRAPHPROMPT+	26.95 \pm 7.42	20.80 \pm 1.45	26.03 \pm 4.17	25.31 \pm 7.65	54.55 \pm 12.61	21.85 \pm 5.15	<u>53.26</u> \pm 14.99	54.73 \pm 14.58
ProNoG	31.54 \pm 5.30	20.92 \pm 1.37	28.50 \pm 5.30	27.17 \pm 9.58	<u>56.11</u> \pm 10.19	22.55 \pm 6.70	<u>51.62</u> \pm 14.27	56.46 \pm 14.57

Table 4: Ablation study on the effects of key components.

Methods	Node classification						Graph classification					
	Wisconsin	Squirrel	Chameleon	PROTEINS	ENZYMEs	Citeseer	Wisconsin	Squirrel	Chameleon	PROTEINS	ENZYMEs	COX2
NO_PROMPT	25.41 \pm 3.13	20.60 \pm 1.30	22.71 \pm 3.54	47.22 \pm 11.05	66.59 \pm 19.28	43.12 \pm 9.61	20.85 \pm 6.74	20.18 \pm 1.30	22.34 \pm 4.15	53.61 \pm 8.90	21.85 \pm 6.17	54.29 \pm 17.31
SINGLE_PROMPT	32.76 \pm 5.21	20.85 \pm 1.32	22.78 \pm 3.35	30.33 \pm 19.59	65.32 \pm 21.67	48.64 \pm 10.09	25.77 \pm 6.24	20.68 \pm 0.91	27.03 \pm 3.98	56.35 \pm 10.59	19.38 \pm 7.12	47.24 \pm 15.53
NODECOND	35.56 \pm 4.65	21.26 \pm 3.95	21.13 \pm 2.23	36.01 \pm 19.70	68.54 \pm 19.31	48.30 \pm 10.22	25.30 \pm 4.62	20.98 \pm 1.56	27.24 \pm 5.24	56.61 \pm 10.03	20.70 \pm 6.67	55.92 \pm 14.66
PRONoG\ SIM	30.65 \pm 4.05	20.05 \pm 0.59	20.96 \pm 4.21	33.73 \pm 17.82	36.02 \pm 20.64	18.74 \pm 2.66	22.05 \pm 5.86	19.93 \pm 0.42	20.20 \pm 1.11	52.30 \pm 10.94	16.70 \pm 1.28	50.05 \pm 17.67
PRONoG	44.72 \pm 11.93	24.59 \pm 3.41	30.67 \pm 3.73	48.95 \pm 10.85	72.94 \pm 20.23	49.02 \pm 10.66	31.54 \pm 5.30	20.92 \pm 1.37	28.50 \pm 5.30	56.11 \pm 10.19	22.55 \pm 6.70	56.46 \pm 14.57

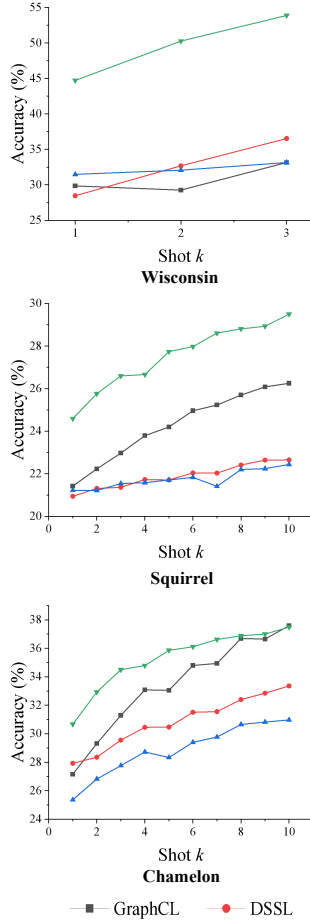
Wisconsin and Cornell, we only conduct tasks up to 3-shot. We observe that: (1) ProNoG significantly outperforms all baselines in low-shot scenarios with very limited labeled data (e.g., $k \leq 5$), showcasing the effectiveness of our approach in these situations. (2) As the number of shots increases, all methods generally show improved performance as expected. However, ProNoG remains competitive and often surpasses the other methods, demonstrating the robustness of ProNoG.

6.3 Ablation Study

To comprehensively understand the influence of conditional prompting in ProNoG, we perform an ablation study comparing ProNoG with four of its variants: NO_PROMPT replaces conditional prompting with a classifier for downstream adaptation. SINGLE_PROMPT uses a single prompt instead of conditional prompting to modify all nodes. NODECOND directly uses the output embedding of the pre-trained graph encoder as input to the condition-net to generate the prompt without reading out the subgraph in Eq. 7. ProNoG\|SIM readout

Table 5: Comparison between homophily and non-homophily pre-training.

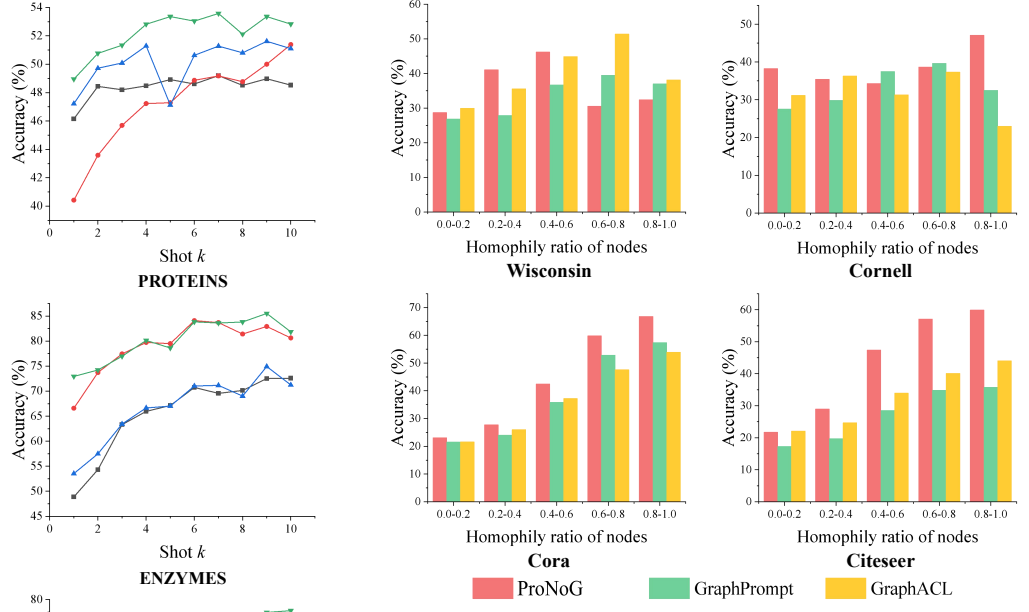
Pre-training task	Node classification				Graph classification			
	Wisconsin 0.21	Cornell 0.30	PROTEINS 0.66	ENZYME 0.67	Wisconsin 0.21	Cornell 0.30	PROTEINS 0.66	ENZYME 0.67
LINK PREDICTION [42]	23.01±11.40	26.27± 7.61	35.88± 5.41	36.74± 2.61	20.96± 4.21	25.38± 2.50	51.50± 6.02	17.47± 4.04
LINK PREDICTION [26]	28.93±11.74	16.29± 7.93	48.95±10.85	52.87±14.73	23.15± 5.67	22.05±13.80	55.83±10.87	22.23± 5.51
GRAPHACL [55]	33.91± 9.04	29.55±12.30	44.08±10.03	50.57±13.11	26.42± 7.25	26.15± 3.87	54.15±10.58	21.64± 5.88
GRAPHCL [60]	44.72±11.93	37.90± 9.31	48.28±11.09	51.46±13.93	31.54± 1.37	27.17± 5.30	53.91± 5.51	21.78±12.12

**Figure 3: Impacts of different shots on node classification.**

the subgraph via mean-pooling without similarity between central nodes and their neighbors as in Eq. 7. As shown in Table 4, ProNoG consistently outperforms or is at least competitive with these variants. This highlights the necessity of readout subgraphs weighted by similarity to capture nodes' non-homophilic patterns, and the advantages of using conditional prompting to specifically characterize nodes.

6.4 Analysis on Pre-Training Methods

To further evaluate homophily and non-homophily tasks, using ProNoG for downstream adaptation, we employ homophily tasks

**Figure 4: Results on different node patterns.**

link prediction used in GraphPrompt [26], and non-homophily tasks GraphCL [60] and DSSL [54], respectively. Note that link prediction in GPPT [42] is in a generative format, thus falling beyond the scope of homophily task, but it's also affected by non-homophily in graphs. We compare these pretext tasks and show the results in Table 5. We observe that for graphs with a low homophily ratio, the non-homophily task significantly outperforms the homophily tasks. Conversely, for graphs with a high homophily ratio, the results of these two methods are mixed, with each having their own strengths and weaknesses.

6.5 Analysis on Varying Node Patterns

To evaluate the ability of ProNoG in capturing node-specific patterns, we calculate the accuracy on different node groups with varying homophily ratios, i.e., [0.0, 0.2), [0.2, 0.4), [0.4, 0.6), [0.6, 0.8), [0.8, 1.0]. We compare ProNoG with several competitive baselines and present the results in Fig. 4. We observe that ProNoG consistently outperforms or is at least competitive with all baselines across all node patterns, regardless of their homophily ratio. These results further demonstrate the effectiveness of ProNoG in capturing node-specific patterns and highlight the advantages of our proposed conditional prompting.

7 Conclusions

In this paper, we explored pre-training and prompt learning on non-homophilic graphs. The objectives are twofold: learning comprehensive knowledge irrespective of the varying non-homophily characteristics of graphs, and adapting the nodes with diverse distributions of non-homophily patterns to downstream applications in a fine-grained, node-wise manner. We first revisit graph pre-training on non-homophilic graphs, providing theoretical insights into the choice of pre-training tasks. Then, for downstream adaptation, we proposed condition-net to generate a series of prompts conditioned on various non-homophilic patterns across nodes. Finally, we conducted extensive experiments on ten public datasets, demonstrating that PRONoG significantly outperforms diverse state-of-the-art baselines.

References

[1] Hangbo Bao, Li Dong, Songhao Piao, and Furu Wei. 2022. BEiT: BERT Pre-Training of Image Transformers. In *ICLR*.

[2] Deyu Bo, Xiao Wang, Chuan Shi, and Huawei Shen. 2021. Beyond low-frequency information in graph convolutional networks. In *AAAI*. 3950–3957.

[3] Karsten M Borgwardt, Cheng Soon Ong, Stefan Schönauer, SVN Vishwanathan, Alex J Smola, and Hans-Peter Kriegel. 2005. Protein function prediction via graph kernels. *Bioinformatics* 21, suppl_1 (2005), i47–i56.

[4] Tom Brown, Benjamin Mann, Nick Ryder, Melanie Subbiah, Jared D Kaplan, Prafulla Dhariwal, Arvind Neelakantan, Pranav Shyam, Girish Sastry, Amanda Askell, et al. 2020. Language models are few-shot learners. *NeurIPS* 33 (2020), 1877–1901.

[5] Mouxiang Chen, Zemin Liu, Chenghao Liu, Jundong Li, Qiheng Mao, and Jianling Sun. 2023. Ultra-dp: Unifying graph pre-training with multi-task graph dual prompt. *arXiv preprint arXiv:2310.14845* (2023).

[6] Li Dong, Nan Yang, Wenhui Wang, Furu Wei, Xiaodong Liu, Yu Wang, Jianfeng Gao, Ming Zhou, and Hsiao-Wuen Hon. 2019. Unified language model pre-training for natural language understanding and generation. *NeurIPS* 32 (2019).

[7] Taoran Fang, Yunchao Zhang, Yang Yang, Chunping Wang, and Lei Chen. 2024. Universal prompt tuning for graph neural networks. *NeurIPS* (2024).

[8] Chelsea Finn, Pieter Abbeel, and Sergey Levine. 2017. Model-agnostic meta-learning for fast adaptation of deep networks. In *ICML*. 1126–1135.

[9] Tianyu Gao, Adam Fisch, and Danqi Chen. 2021. Making Pre-trained Language Models Better Few-shot Learners. In *ACL*. 3816–3830.

[10] David Ha, Andrew Dai, and Quoc V Le. 2016. Hypernetworks. *arXiv preprint arXiv:1609.09106* (2016).

[11] Will Hamilton, Zhitao Ying, and Jure Leskovec. 2017. Inductive representation learning on large graphs. *NeurIPS* (2017), 1025–1035.

[12] Kaveh Hassani and Amir Hosein Khasahmadi. 2020. Contrastive multi-view representation learning on graphs. In *ICML*. 4116–4126.

[13] Dongxiao He, Jitao Zhao, Rui Guo, Zhiyong Feng, Di Jin, Yuxiao Huang, Zhen Wang, and Weixiong Zhang. 2023. Contrastive learning meets homophily: two birds with one stone. In *International Conference on Machine Learning*. 12775–12789.

[14] Weihua Hu, Bowen Liu, Joseph Gomes, Marinka Zitnik, Percy Liang, Vijay Pande, and Jure Leskovec. 2020. Strategies for Pre-training Graph Neural Networks. In *ICLR*.

[15] Ziniu Hu, Yuxiao Dong, Kuansan Wang, Kai-Wei Chang, and Yizhou Sun. 2020. GPT-GNN: Generative pre-training of graph neural networks. In *SIGKDD*. 1857–1867.

[16] Shuo Ji, Xiaodong Lu, Mingzhe Liu, Leilei Sun, Chuanren Liu, Bowen Du, and Hui Xiong. 2023. Community-based dynamic graph learning for popularity prediction. In *SIGKDD*. 930–940.

[17] Wei Jin, Tyler Derr, Yiqi Wang, Yao Ma, Zitao Liu, and Jiliang Tang. 2021. Node similarity preserving graph convolutional networks. In *WSDM*. 148–156.

[18] Anshul Kanakia, Zhihong Shen, Darrin Eide, and Kuansan Wang. 2019. A scalable hybrid research paper recommender system for microsoft academic. In *WWW*. 2893–2899.

[19] Thomas N Kipf and Max Welling. 2016. Variational graph auto-encoders. In *Bayesian Deep Learning Workshop*.

[20] Thomas N Kipf and Max Welling. 2017. Semi-supervised classification with graph convolutional networks. In *ICLR*.

[21] Namkyeong Lee, Kanghoon Yoon, Gyoung S Na, Sein Kim, and Chanyoung Park. 2023. Shift-robust molecular relational learning with causal substructure. In *SIGKDD*. 1200–1212.

[22] Brian Lester, Rami Al-Rfou, and Noah Constant. 2021. The Power of Scale for Parameter-Efficient Prompt Tuning. In *EMNLP*. 3045–3059.

[23] Pengfei Liu, Weizhe Yuan, Jinlan Fu, Zhengbao Jiang, Hiroaki Hayashi, and Graham Neubig. 2023. Pre-train, prompt, and predict: A systematic survey of prompting methods in natural language processing. *Comput. Surveys* (2023), 1–35.

[24] Xiao Liu, Yanan Zheng, Zhengxiao Du, Ming Ding, Yujie Qian, Zhihui Yang, and Jie Tang. 2021. GPT understands, too. *arXiv preprint arXiv:2103.10385* (2021).

[25] Zemin Liu, Yuan Fang, Chenghao Liu, and Steven CH Hoi. 2021. Relative and absolute location embedding for few-shot node classification on graph. In *AAAI*. 4267–4275.

[26] Zemin Liu, Xingtong Yu, Yuan Fang, and Ximeng Zhang. 2023. GraphPrompt: Unifying pre-training and downstream tasks for graph neural networks. In *WWW*. 417–428.

[27] Yuanfu Lu, Xunqiang Jiang, Yuan Fang, and Chuan Shi. 2021. Learning to pre-train graph neural networks. In *AAAI*. 4276–4284.

[28] Sitao Luan, Chenqing Hua, Qincheng Lu, Jiaqi Zhu, Mingde Zhao, Shuyuan Zhang, Xiao-Wen Chang, and Doina Precup. 2022. Revisiting heterophily for graph neural networks. *Advances in neural information processing systems* (2022), 1362–1375.

[29] Yao Ma, Xiaorui Liu, Neil Shah, and Jiliang Tang. 2022. Is homophily a necessity for graph neural networks?. In *ICLR*.

[30] Haitao Mao, Zhikai Chen, Wei Jin, Haoyu Han, Yao Ma, Tong Zhao, Neil Shah, and Jiliang Tang. 2023. Demystifying structural disparity in graph neural networks: Can one size fit all?. In *NeurIPS*.

[31] Andrew Kachites McCallum, Kamal Nigam, Jason Rennie, and Kristie Seymore. 2000. Automating the construction of internet portals with machine learning. *Information Retrieval* (2000).

[32] Trung-Kien Nguyen and Yuan Fang. 2024. Diffusion-based Negative Sampling on Graphs for Link Prediction. In *WWW*. 948–958.

[33] Hongbin Pei, Bingzhe Wei, Kevin Chen-Chuan Chang, Yu Lei, and Bo Yang. 2020. Geom-gcn: Geometric graph convolutional networks. *arXiv preprint arXiv:2002.05287* (2020).

[34] Zhen Peng, Wenbing Huang, Minnan Luo, Qinghua Zheng, Yu Rong, Tingyang Xu, and Junzhou Huang. 2020. Graph representation learning via graphical mutual information maximization. In *WWW*. 259–270.

[35] Oleg Platonov, Denis Kuznecov, Michael Diskin, Artem Babenko, and Liudmila Prokhorenkova. 2023. A critical look at the evaluation of GNNs under heterophily: Are we really making progress?. In *ICLR*.

[36] Jiezhong Qiu, Qibin Chen, Yuxiao Dong, Jing Zhang, Hongxia Yang, Ming Ding, Kuansan Wang, and Jie Tang. 2020. GCC: Graph contrastive coding for graph neural network pre-training. In *SIGKDD*. 1150–1160.

[37] Faisal Rahutomo, Teruaki Kitasaka, Masayoshi Arisugi, et al. 2012. Semantic cosine similarity. In *ICAST*.

[38] Ryan A. Rossi and Nesreen K. Ahmed. 2015. The Network Data Repository with Interactive Graph Analytics and Visualization. In *AAAI*. 4292–4293.

[39] Benedek Rozemberczki, Carl Allen, and Rik Sarkar. 2021. Multi-scale attributed node embedding. *Journal of Complex Networks* (2021), cnab014.

[40] Timo Schick and Hinrich Schütze. 2021. It's Not Just Size That Matters: Small Language Models Are Also Few-Shot Learners. In *NAACL*. 2339–2352.

[41] Prithviraj Sen, Galileo Namata, Mustafa Bilgic, Lise Getoor, Brian Galligher, and Tina Eliassi-Rad. 2008. Collective classification in network data. *AI magazine* (2008).

[42] Mingchen Sun, Kaixiong Zhou, Xin He, Ying Wang, and Xin Wang. 2022. GPPT: Graph Pre-training and Prompt Tuning to Generalize Graph Neural Networks. In *SIGKDD*. 1717–1727.

[43] Xiangguo Sun, Hong Cheng, Jia Li, Bo Liu, and Jihong Guan. 2023. All in One: Multi-Task Prompting for Graph Neural Networks. In *SIGKDD*.

[44] Xiangguo Sun, Jiawen Zhang, Xixi Wu, Hong Cheng, Yun Xiong, and Jia Li. 2023. Graph prompt learning: A comprehensive survey and beyond. *arXiv preprint arXiv:2311.16534* (2023).

[45] Shiyin Tan, Dongyuan Li, Renhe Jiang, Ying Zhang, and Manabu Okumura. 2024. Community-Invariant Graph Contrastive Learning. In *ICML*.

[46] Zhen Tan, Ruocheng Guo, Kaize Ding, and Huan Liu. 2023. Virtual Node Tuning for Few-shot Node Classification. *arXiv preprint arXiv:2306.06063* (2023).

[47] Petar Veličković, Guillem Cucurull, Arantxa Casanova, Adriana Romero, Pietro Liò, and Yoshua Bengio. 2018. Graph attention networks. In *ICLR*.

[48] Petar Veličković, William Fedus, William L Hamilton, Pietro Liò, Yoshua Bengio, and R Devon Hjelm. 2019. Deep Graph Infomax. In *ICLR*.

[49] Ning Wang, Minnan Luo, Kaize Ding, Lingling Zhang, Jundong Li, and Qinghua Zheng. 2020. Graph few-shot learning with attribute matching. In *CIKM*. 1545–1554.

[50] Song Wang, Yushun Dong, Xiao Huang, Chen Chen, and Jundong Li. 2022. FAITH: Few-Shot Graph Classification with Hierarchical Task Graphs. In *IJCAI*.

[51] Xu Wang, Huan Zhao, Wei-wei Tu, and Quanming Yao. 2023. Automated 3D pre-training for molecular property prediction. In *SIGKDD*. 2419–2430.

[52] Yuzhong Wu and Tan Lee. 2018. Reducing model complexity for DNN based large-scale audio classification. In *ICASSP*. 331–335.

[53] Zonghan Wu, Shirui Pan, Fengwen Chen, Guodong Long, Chengqi Zhang, and S Yu Philip. 2020. A comprehensive survey on graph neural networks. *TNNLS* 32, 1 (2020), 4–24.

[54] Teng Xiao, Zhengyu Chen, Zhimeng Guo, Zeyang Zhuang, and Suhang Wang. 2022. Decoupled self-supervised learning for graphs. *NeurIPS* (2022), 620–634.

[55] Teng Xiao, Huaiseng Zhu, Zhengyu Chen, and Suhang Wang. 2023. Simple and asymmetric graph contrastive learning without augmentations. *Advances in Neural Information Processing Systems* (2023).

[56] Chenyan Xiong, Russell Power, and Jamie Callan. 2017. Explicit semantic ranking for academic search via knowledge graph embedding. In *WWW*. 1271–1279.

[57] Keyulu Xu, Weihua Hu, Jure Leskovec, and Stefanie Jegelka. 2019. How powerful are graph neural networks?. In *ICLR*.

[58] Yujun Yan, Milad Hashemi, Kevin Swersky, Yaoqing Yang, and Dana Koutra. 2022. Two sides of the same coin: Heterophily and oversmoothing in graph convolutional neural networks. In *ICDM*. 1287–1292.

[59] Chengxuan Ying, Tianhe Cai, Shengjie Luo, Shuxin Zheng, Guolin Ke, Di He, Yanming Shen, and Tie-Yan Liu. 2021. Do transformers really perform badly for graph representation?. In *NeurIPS*. 28877–28888.

[60] Yuning You, Tianlong Chen, Yongduo Sui, Ting Chen, Zhangyang Wang, and Yang Shen. 2020. Graph contrastive learning with augmentations. *NeurIPS* 33 (2020), 5812–5823.

- [61] Xingtong Yu, Yuan Fang, Zemin Liu, Yuxia Wu, Zhihao Wen, Jianyuan Bo, Xinxing Zhang, and Steven CH Hoi. 2024. Few-Shot Learning on Graphs: from Meta-learning to Pre-training and Prompting. *arXiv preprint arXiv:2402.01440* (2024).
- [62] Xingtong Yu, Zhenghao Liu, Yuan Fang, Zemin Liu, Sihong Chen, and Xinming Zhang. 2024. Generalized graph prompt: Toward a unification of pre-training and downstream tasks on graphs. *IEEE Transactions on Knowledge and Data Engineering* (2024).
- [63] Xingtong Yu, Zemin Liu, Yuan Fang, and Xinming Zhang. 2023. Learning to count isomorphisms with graph neural networks. In *AAAI*.
- [64] Xingtong Yu, Zemin Liu, Yuan Fang, and Xinming Zhang. 2024. HG_PROMPT: Bridging Homogeneous and Heterogeneous Graphs for Few-shot Prompt Learning. In *AAAI*.
- [65] Xingtong Yu, Chang Zhou, Yuan Fang, and Xinming Zhang. 2024. MultiGPrompt for Multi-Task Pre-Training and Prompting on Graphs. In *WWW*.
- [66] Seongjun Yun, Minbyul Jeong, Raehyun Kim, Jaewoo Kang, and Hyunwoo J Kim. 2019. Graph transformer networks. *NeurIPS* 32 (2019).
- [67] Yuhang Zang, Wei Li, Kaiyang Zhou, Chen Huang, and Chen Change Loy. 2022. Unified vision and language prompt learning. *arXiv preprint arXiv:2210.07225* (2022).
- [68] Shiqi Zhang, Yiqian Huang, Jiachen Sun, Wenqing Lin, Xiaokui Xiao, and Bo Tang. 2023. Capacity constrained influence maximization in social networks. In *SIGKDD*. 3376–3385.
- [69] Fan Zhou, Chengtai Cao, Kumpeng Zhang, Goce Trajcevski, Ting Zhong, and Ji Geng. 2019. Meta-GNN: On few-shot node classification in graph meta-learning. In *CIKM*. 2357–2360.
- [70] Jie Zhou, Ganqiu Cui, Shengding Hu, Zhengyan Zhang, Cheng Yang, Zhiyuan Liu, Lifeng Wang, Changcheng Li, and Maosong Sun. 2020. Graph neural networks: A review of methods and applications. *AI open* (2020), 57–81.
- [71] Kaiyang Zhou, Jingkang Yang, Chen Change Loy, and Ziwei Liu. 2022. Conditional prompt learning for vision-language models. In *CVPR*. 16816–16825.
- [72] Kaiyang Zhou, Jingkang Yang, Chen Change Loy, and Ziwei Liu. 2022. Learning to prompt for vision-language models. *IJCV* (2022), 2337–2348.
- [73] Jiong Zhu, Junchen Jin, Donald Loveland, Michael T Schaub, and Danai Koutra. 2022. How does heterophily impact the robustness of graph neural networks? theoretical connections and practical implications. In *SIGKDD*. 2637–2647.
- [74] Jiong Zhu, Ryan A Rossi, Anup Rao, Tung Mai, Nedim Lipka, Nesreen K Ahmed, and Danai Koutra. 2021. Graph neural networks with heterophily. In *AAAI*. 11168–11176.
- [75] Jiong Zhu, Yujun Yan, Lingxiao Zhao, Mark Heimann, Leman Akoglu, and Danai Koutra. 2020. Beyond homophily in graph neural networks: Current limitations and effective designs. *NeurIPS* (2020), 7793–7804.
- [76] Yanqiao Zhu, Yichen Xu, Feng Yu, Qiang Liu, Shu Wu, and Liang Wang. 2020. Deep graph contrastive representation learning. *arXiv preprint arXiv:2006.04131* (2020).

Appendices

A Algorithm

We detail the main steps for conditional prompt generation and tuning in Algorithm 1. In brief, we iterate through each downstream task to learn the corresponding prompt vectors individually. In lines 3–5, we compute the embedding for each node using the pre-trained graph encoder, with the pre-trained weights Θ_0 remaining fixed throughout the adaptation process. In lines 8–22, we optimize the condition-net. Specifically, we perform similarity-weighted readout (lines 9–11), generate prompts (lines 12–13), modify nodes’ embeddings using these prompts (lines 12–15), and update the embeddings for the prototypical nodes/graphs based on the few-shot labeled data provided in the task (lines 18–19). Note that updating prototypical nodes/graphs is necessary only for classification tasks.

B Homophily and Non-Homophily Methods

We provide further details about the set of positive samples \mathcal{A} and negative samples \mathcal{B} of homophily and non-homophily methods in Table 5.

C Further Descriptions of Datasets

We conduct experiments on ten benchmark datasets.

- *Wisconsin*³ [33] is a network of 251 nodes, where each node stands for a webpage, and 199 edges signify the hyperlinks connecting these pages. The features of the nodes are derived from a bag-of-words representation of the webpages. These pages are manually classified into five categories: student, project, course, staff, and faculty. The edge homophily ratio is 0.21.
- *Cornell*⁴ [33] is also a webpage network. It comprises 183 nodes, each symbolizing a webpage, and 295 edges, which represent the hyperlinks between these pages. The node features are obtained from a bag-of-words representation of the webpages. These pages are manually sorted into five categories: student, project, course, staff, and faculty. The edge homophily ratio is 0.22.
- *Chameleon*⁵ [39] is a Wikipedia network, consisting of 2,277 Wikipedia pages. The pages are divided into five categories according to their average monthly traffic. This dataset creates a network of pages with 36,101 connections, and the node features consist of various key nouns extracted from the Wikipedia pages. The edge homophily ratio is 0.23.
- *Squirrel*⁶ [39] comprises 5,201 Wikipedia web pages of discussing the defined topics. The dataset is also divided into five categories according to their average monthly traffic. This dataset is a page-page network with 217,073 edges, and the node features are based on several informative nouns in the Wikipedia pages. The edge homophily ratio is 0.30.
- *PROTEINS*⁷ [3] comprises a dataset of protein graphs, reflecting various characteristics such as amino acid sequences, conformations, structures, and unique features like active

³https://github.com/bingzhewei/geom-gcn/tree/master/new_data/wisconsin

⁴https://github.com/bingzhewei/geom-gcn/tree/master/new_data/cornell

⁵https://github.com/Sitaoluan/ACM-GNN/tree/main/new_data/chameleon

⁶https://github.com/Sitaoluan/ACM-GNN/tree/main/new_data/squirrel

⁷<https://www.chrsmrrs.com/graphkerneldatasets/PROTEINS.zip>

sites. In this dataset, each node represents a secondary structure, and each edge signifies a neighboring relationship either within the amino acid sequence or in three-dimensional space. Nodes are classified into three categories, while the graphs themselves are divided into two classes. The edge homophily ratio is 0.66.

- *ENZYME*⁸ [50] is a collection of 600 enzymes, sourced from the BRENDA enzyme database. The enzymes are divided into 6 different classes, following their top-level EC enzyme classification. The edge homophily ratio is 0.67.
- *CiteSeer*⁹ [41] contains 3,312 scientific papers, divided into six different categories. The dataset includes a citation network with 4,732 edges. Each paper is represented by a binary word vector, indicating the presence or absence of each word from a dictionary comprising 3,703 unique terms. The edge homophily ratio is 0.74.
- *Cora*¹⁰ [31] includes 2,708 scientific papers, divided into seven distinct categories. The dataset features a citation network with 5,429 edges. Each paper is represented by a binary word vector, indicating whether each of the 1,433 unique words from the dictionary is present or absent. The edge homophily ratio is 0.81.
- *BZR*¹¹ [38] comprises a dataset of 405 ligands linked to the benzodiazepine receptor, represented as individual graph structures. These ligands are divided into 2 distinct categories.
- *COX2*¹² [38] consists of a dataset of 467 molecular structures representing cyclooxygenase-2 inhibitors. In this dataset, each node corresponds to an atom and each edge denotes a chemical bond—single, double, triple, or aromatic—between atoms. The molecules are classified into two categories.

D Further Descriptions of Baselines

In this section, we present more details for the baselines used in our experiments.

(1) End-to-end Graph Neural Networks

- **GCN** [20]: GCN utilizes a mean-pooling strategy for neighborhood aggregation to integrate information from neighboring nodes.
- **GAT** [47]: GAT also leverages neighborhood aggregation for end-to-end node representation learning, uniquely assigns varying attention weights to different neighbors, thereby adjusting their impact on the aggregation process.
- **H2GCN** [75]: H2GCN improves node classification by separating ego- and neighbor-embeddings, using higher-order neighborhoods, and combining intermediate representations. These designs help it perform well on both homophilous and heterophilous graphs.
- **FAGCN** [2]: FAGCN improves node representation by adaptively combining low- and high-frequency signals using a self-gating mechanism, making it effective for different network types and reducing over-smoothing.

⁸<http://www.chrsmrrs.com/graphkerneldatasets/ENZYME.zip>

⁹<https://nrvs.com/download/data/labeled/citeSeer.zip>

¹⁰<https://relational.fit.cvut.cz/dataset/CORA>

¹¹<https://www.chrsmrrs.com/graphkerneldatasets/BZR.zip>

¹²<https://www.chrsmrrs.com/graphkerneldatasets/COX2.zip>

Table 6: Positive and negative samples for homophily and non-homophily methods.

Pre-training task	Positive instances \mathcal{A}_u	Negative instances \mathcal{B}_u	Homophily task
Link prediction [26, 62, 64]	a node connected to node u	nodes disconnected to node u	Yes
DGI [48]	nodes in graph G	nodes in corrupted graph G'	No
GraphCL [60]	an augmented graph from graph G	augmented graphs from $G' \neq G$	No
GraphACL [55]	nodes with similar ego-subgraph to node u	nodes with dissimilar ego-subgraph to node u	No

Algorithm 1 CONDITIONAL PROMPT LEARNING FOR ProNoG

Input: Pre-trained graph encoder with parameters Θ_0 ,
1: a set of downstream tasks $\mathcal{T} = \{t_1, \dots, t_n\}$.
Output: Optimized parameters $\{\phi_{t_1}, \dots, \phi_{t_n}\}$ of n condition-nets

```

2: for  $i \leftarrow 1$  to  $n$  do
3:   /* Encoding graphs via pre-trained graph encoder */
4:   for each graph  $G = (V, E, X)$  in task  $t_i$  do
5:      $H \leftarrow \text{GRAPHENCODER}(G; \Theta_0)$ 
6:      $h_v \leftarrow H[v]$ , where  $v$  is a node in  $G$ 
7:      $\phi_i \leftarrow \text{initialization}$ 
8:     while not converged do
9:       for each node  $v \in V$  in task  $t_i$  do
10:        /* Subgraph sampling and readout Eq. (7) */
11:        Sample  $v$ 's  $k$ -hop subgraph  $S_v$ 
12:         $s_v \leftarrow \text{AVERAGE}(\{\mathbf{h}_u \cdot \text{sim}(\mathbf{h}_u, \mathbf{h}_v) : u \in V(S_v)\})$ 
13:        /* Generate pattern-based prompts by Eq. (8) */
14:         $\mathbf{p}_{t_i, v} \leftarrow \text{CONDNET}(s_v; \phi_{t_i})$ 
15:        /* Prompt modification by Eq. (9) */
16:         $\tilde{\mathbf{h}}_{t_i, v} \leftarrow \mathbf{p}_{t_i, v} \odot \mathbf{h}_v$ 
17:         $\mathbf{h}_{t_i, G} = \text{AVERAGE}(\tilde{\mathbf{h}}_{t_i, v} : v \in \mathcal{V})$ 
18:        /* Update prototypical subgraphs */
19:        for each class  $c$  in task  $t_i$  do
20:           $\mathbf{h}_{t_i, c} \leftarrow \text{AVERAGE}(\tilde{\mathbf{h}}_{t_i, x} : \text{instance } x \text{ belongs to class } c)$ 
21:        /* Optimizing the parameters in condition-net */
22:        Calculate  $\mathcal{L}_{\text{down}}(\phi_i)$  by Eq. (10)
23:        Update  $\phi_i$  by backpropagating  $\mathcal{L}_{\text{down}}(\phi_i)$ 
24: return  $\{\phi_{t_1}, \dots, \phi_{t_n}\}$ 

```

(2) Graph Pre-training Models

- **DGI** [47]: DGI operates as a self-supervised pre-training methodology tailored for homogeneous graphs. It is predicated on the maximization of mutual information (MI), aiming to enhance the estimated MI between locally augmented instances and their global counterparts.
- **GraphCL** [60]: GraphCL leverages a variety of graph augmentations for self-supervised learning, tapping into the intrinsic structural patterns of graphs. The overarching goal is to amplify the concordance between different augmentations throughout graph pre-training.
- **DSSL** [54]: DSSL uses latent variable modeling to decouple semantics in neighborhoods, avoiding augmentations and optimizing with variational inference to capture local and global information, enhancing node representation learning.
- **GraphACL** [55]: GraphACL considers each node from two perspectives: identity representation and context representation. The model trains the former by predicting the context representation of one-hop neighbors using an asymmetric predictor, and then reconstructs the same latter of the central

node by enforcing identity representations from two-hop neighbors.

(3) Graph Prompt Models

- **GPPT** [42]: GPPT utilizes a GNN model pre-trained via a link prediction task which is a strong homophily method. The downstream prompt module is designed specifically for node classification, aligning it with the pre-training link prediction task.
- **GraphPrompt** [26]: GraphPrompt employs subgraph similarity calculations as a unified template to bridge the gap between pre-training and downstream tasks, including node and graph classification. A learnable prompt is fine-tuned during downstream adaptation to incorporate task-specific knowledge.
- **GraphPrompt+** [62]: GraphPrompt+ builds on GraphPrompt by introducing a series of prompt vectors within each layer of the pre-trained graph encoder. This technique utilizes hierarchical information from multiple layers, beyond just the readout layer.

E Implementation Details of Approaches

General settings Optimizer. For all experiments, we use the Adam optimizer.

Environment. The environment in which we run experiments is:

- Linux version: 5.15.0-78-generic
- Operating system: Ubuntu 18.04.5 LTS
- CPU information: Intel(R) Xeon(R) Platinum 8352V
- GPU information: GeForce RTX 4090 (24 GB)

Details of baselines. We use the official code provided for all open-source baselines. Each model is tuned according to the settings recommended in their respective publications to ensure optimal performance. We use early stopping strategy for training and set patience to 50 steps. The number of training epochs is set to 2,000.

- For the baseline GCN [20], we employ a 3-layer architecture on Wisconsin, Squirrel, Chameleon, Cornell datasets and 2-layer architecture on Cora, Citeseer, ENZYMES, PROTEINS, COX2, BZR datasets. Hidden dimensions is 256.
- For GAT [47], we employ a 2-layer architecture and set the hidden dimension to 256. Additionally, we apply 8 attention heads in the first GAT layer.
- For H2GCN [75], we employ a 2-layer architecture and set the hidden dimension to 256.
- For FAGCN [2], we employ a 2-layer architecture. The hyper-parameter setting is: $\text{eps} = 0.3$, $\text{dropout} = 0.5$, $\text{hidden} = 256$. we use relu as activation function.

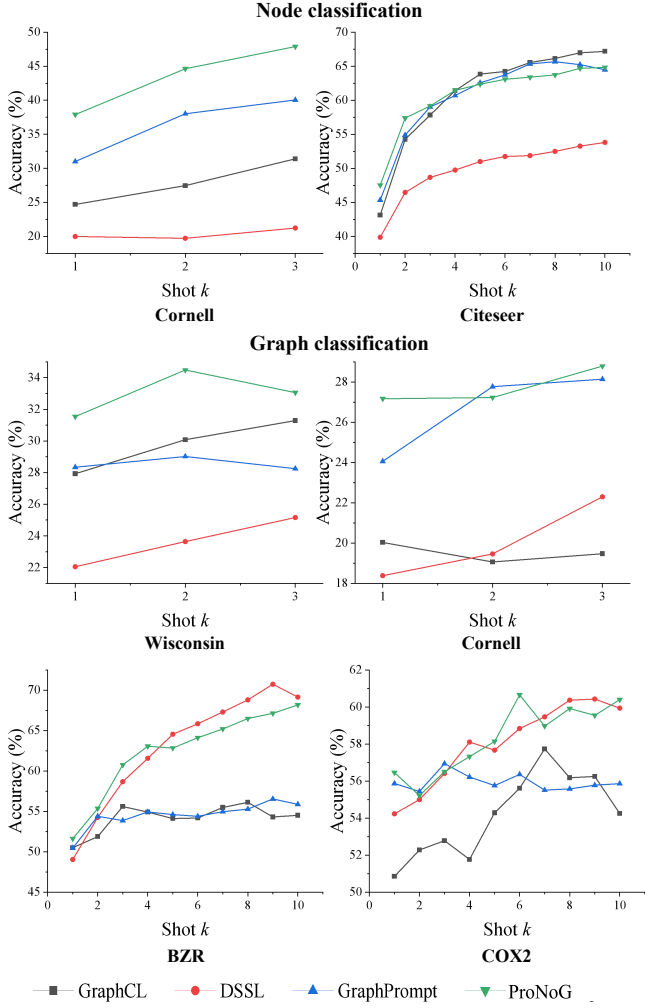


Figure 5: Impacts of different shots on node and graph classification.

- For DGI [47], we utilize a 1-layer GCN as the base model and set the hidden dimensions to 256. Additionally, we employ prelu as the activation function.
- For GraphCL [60], a 1-layer GCN is also employed as its base model, with the hidden dimensions set to 256. Specifically, we select edge dropping as the augmentations, with a default augmentation ratio of 0.2.
- For DSSL [54], the hidden dimension search space is in {64, 256, 2048}. We report the best performance on PROTEINS and ENZYMEs with hidden size of 64, Cora and Citeseer with 2048, and the rest datasets with 256. We keep the other hyper-parameters the same as in the original demonstrations in their Github repository.
- For GraphACL [55], the hidden dimension search space is in {64, 256, 1024, 2048}. We report the best performance on PROTEINS and ENZYMEs with hidden size of 64, Cora and Citeseer with 2048, and the rest datasets with 256. We

Table 7: Comparison of the number of tunable parameters during the downstream adaptation phase.

Methods	Wisconsin	Chameleon	Citeseer	Cora
GCN	501,504	660,736	947,968	366,848
FAGCN	440,654	601,130	956,654	370,994
GRAPHCL	1,280	1,280	1,536	1,792
GRAPHACL	1,280	1,280	12,288	14,336
GRAPHPROMPT	256	256	256	256
GRAPHPROMPT+	512	512	512	512
ProNoG	1,024	1,024	1,024	1,024

keep the other hyper-parameters the same as in the original demonstrations in their Github repository.

- For GPPT [42], we utilize a 2-layer GraphSAGE as its base model, setting the hidden dimensions to 256. For base GraphSAGE, we also employ a mean aggregator.
- For GraphPrompt [26], we employ a 3-layer architecture on Wisconsin, Squirrel, Chameleon, Cornell datasets and 2-layer architecture on Cora, Citeseer, ENZYMEs, PROTEINS, COX2, BZR datasets. Hidden dimensions are set to 256.
- For GraphPrompt+ [62], we employ a 2-layer GCN on Cora, Citeseer, ENZYMEs, PROTEINS, COX2, BZR datasets and 3-layer GCN on the rest datasets. Hidden dimensions are set to 256.

Details of ProNoG. For our proposed ProNoG, we utilize a 2-layer FAGCN architecture as backbone for pre-training task with graph contrastive methods for Wisconsin, Squirrel, Chameleon, Cornell. Especially, we implement edge-dropping on sub-graph level for Wisconsin, Squirrel, Chameleon, Cornell. Hidden dimensions are set to 256. For Cora, Citeseer, BZR, COX2, we employ 1-layer GCN as base model for pre-training task. Hidden dimensions are set to 256. For PROTEINS, we employ 1-layer GCN on link prediction task for pre-training. Hidden dimensions is set to 64. For ENZYMEs, we implement DSSL for pretraining. Hidden dimensions is set to 64. All experiments are undertaken with the seed of 39. Especially, we found that on Chameleon, Squirrel, keeping the original node features as input without normalization performs the best, while for others, normalization of node features remains routine. Except for DSSL, we use cosine-similarity loss on node level as loss function.

F Impact of Shots

We vary the number of shots and conduct node classification on *Cornell* and *Citeseer*, and graph classification tasks on *Wisconsin*, *Cornell*, *BZR* and *COX2*. The results are illustrated in Fig. 5, and we observe same patterns as shown in node classification tasks on other datasets.

G Parameters efficiency

We evaluate the parameter efficiency of ProNoG compared to other notable methods. Specifically, we evaluate the number of parameters that need to be updated or tuned during the downstream adaptation phase, and present the results in Table 7. For GCN and FAGCN, since these models are trained end-to-end, all

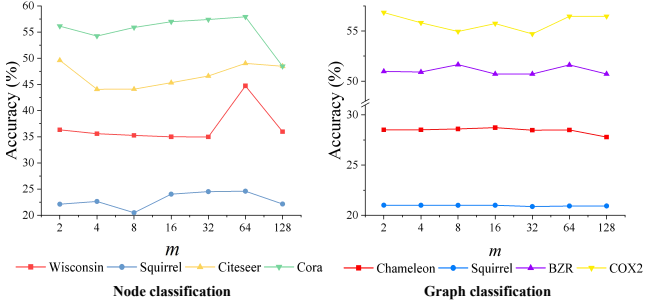


Figure 6: Sensitivity study of m .

model weights must be updated, leading to the lowest parameter efficiency. In contrast, for GraphCL and xxx, only the downstream classifier is updated, while the pre-trained model weights remain unchanged, significantly reducing the number of parameters that require tuning. Prompt-based methods GraphPrompt, GraphPrompt+, and ProNoG are the most parameter-efficient, as prompts or condition-net are lightweight and contain fewer parameters than typical classifiers like fully connected layers. Note that the reported number of parameters for ProNoG are based on $d = 2$, given that ProNoG still performs competitively with such hyperparameter setting. Although our conditional prompt design requires to update more parameters than GraphPrompt and GraphPrompt+ during downstream adaptation, the increase is minor compared to updating the entire classifier or model weights, and thus does not pose a major issue.

H Hyperparameter Analysis

In our experiment, we use a 2-layer MLP with a bottleneck structure as the condition-net. We evaluate the impact of the hidden dimension of the condition-net m and report the corresponding performance in Fig. 6. We observe that for both node and graph classification, as m increases from 2, the performance generally first decreases because a larger m introduces more learnable parameters, which may lead to worse performance in few-shot settings. However, after reaching a trough, accuracy starts to gradually increase as m grows further, since higher dimensions increase model capacity, until reaching a peak. Then the performance further declines as m improves, given more learnable parameters. Note that the overall variation in performance is generally small, and the peak is generally at $m = 2$ or $m = 64$. In our experiment, we set $m = 64$ in our experiments.